PROGRESS
IN COLOR, COLORANTS AND COATINGS

available online @ www.pccc.icrc.ac.ir

Progress in Color Colorants Coating 16 (2023), 47-57

Ministry of Science, Research and Technology
Institute for Color Science & Technology

Corrosion and UV Resistant Coatings Using Fluoroethylene Vinyl Ether Polymer

M. Mirzaee, M. Rezaei Abadchi*, A. Mehdikhani, N. Riahi Noori, A. Zolriasatein
Non-metallic Group, Niroo Research Institute (NRI), P.O. Box: 14665-517, Tehran, Iran

ARTICLE INFO

Article history:
Received: 18 Feb 2021
Final Revised: 22 May 2022
Accepted: 24 May 2022
Available online: 03 Oct 2022

Keywords:
Fluoethylene vinyl ether resin
Coating
Adhesion
Corrosion resistance
UV resistance

ABSTRACT

Among the different methods of preventing corrosion, coatings are the most common method of protecting against corrosion of metallic structures in aggressive environments. Organic coatings provide a barrier between the corrosive environment and the metallic substrate and are one of the most effective and least costly corrosion protection methods. In addition to increasing corrosion resistance, the coating should provide good UV resistance. The polymer fluorethylene vinyl ether (FEVE) was coated to increase corrosion resistance in steel structures. The coating was characterized by electrochemical impedance spectroscopy (EIS), dynamic polarization, adhesion, salt spray, field emission scanning electron microscopy (FESEM), and UV weathering. Results showed that barrier effects were improved and coating resistance increased. As the immersion time increased, the carbon-fluorine linear chains at the surface caused the surface hydrophobicity. The hydrophobicity was not reduced by the increasing immersion time, and even with the presence of corrosion products, an increase in corrosion resistance was observed over time. The adhesion of the FEVE coating to the steel surface is more significant than 100 psi. The 360-hour salt fog test confirmed only blistering on the coating surface and showed no signs of rust around the scratch. This coating had excellent scratch resistance in the B-H range. The weather resistance test also demonstrated the excellent resistance of this UV coating without any change of color and gloss. Prog. Color Colorants Coat. 16 (2023), 47-57© Institute for Color Science and Technology.

1. Introduction

The atmospheric conditions of harsh environments accelerate the corrosion and destruction of structures in various industries, especially metal towers and concrete girders, making them difficult to maintain, repair, and inspect. Generally, corrosion poses a significant threat to the economy, industry, and human life [1-3]. Meanwhile, modified polymeric coatings have been introduced to protect metals from corrosion, which is an appropriate solution for increasing the service life and reducing the cost of maintaining metal equipment. [4-6]. Fluoropolymers are substances that have all or a portion of Olefin hydrogen replaced by fluorine. In polymers such as polytetrafluoroethylene and perfluoroalkoxy alkane, this substitution is complete, and for polymers such as ethylene chloride and ethylene fluoride, this

*Corresponding author: * Mrrezaei@nri.ac.ir
Doi: 10.30509/pccc.2022.166951.1156

substitution is limited. These polymers are highly resistant to various corrosive environments at high temperatures. It is thus widely used in the chemical industry to coat the internal surfaces of the equipment (tanks, towers, pipes and fittings, valves) that are exposed to a variety of corrosive substances. These coatings have the highest chemical and thermal resistance among non-inert coatings. There are different types of fluoropolymers; due to these polymers' other properties and behavior, their coating selection should be made according to the chemical conditions used and the type of equipment relevant experts [7-9].

FEVE polymers have fluoropolymer and hydrocarbon properties, are durable, do not dissolve in solvents, and cannot be used in liquid coatings. These coatings have more properties than other fluorinated polymer resins and can be used in various coatings. FEVE can be used in coating formulations to produce coatings with a wide range of gloss. An ethylene fluorine monomer with a vinyl ether monomer copolymerizes to produce FEVE. Coatings made from them have properties like excellent weather resistance. FEVE resins are used in architectural coatings, industrial, space, and marine coatings. Many bridges, including the Akashi Street Bridge in Japan, used urethane-based FEVE coating. The growing demand for more sustainable coatings has led to the development of FEVE resins [10-12]. This polymer is also essential for water repellency and oil repellency. Shen et al. significantly reduced the corrosion current by coating the FEVE on the steel surface. They attribute the reduction of the corrosion current to protecting the coating barrier from corrosive species [12]. Liu et al. achieved a contact angle above 150 ° and high UV resistance by dispersing graphene oxide and titanium oxide in the FEVE matrix. Preliminary EIS studies on FEVE coatings have shown that while the initial impedance of FEVE chemistry is similar to other coating chemicals, FEVE coatings retain a much higher percentage of the initial impedance after aging and exposure to the elements. FEVE coatings can maintain a strong barrier compared to conventional coatings due to the excellent weathering [13]. Joo et al. also showed that FEVE has good corrosion resistance in the salt spray chamber test after 250 hours. Migration of the fluoride phase towards the surface can be improved by faster crosslinking of this phase [14]. Ghadimi et al. also showed the most efficient coating with superhydrophobicity and high oil repellency. It was produced by the modified FEVE coating with silicon oxide nanoparticles. The results indicated the desorption of water and oil were at a contact angle of 152° and 141° with high adhesion to the substrate, respectively [15]. In this research, the FEVE coating was coated with St37 steel, and its corrosion and weather resistance tests were evaluated.

2. Experimental

2.1. Chemicals and synthesis of coating

Ingredients for this study included FEVE resin and isocyanate curing agent purchased from Changshu Donghuan Chemistry Corporation (Fluorine content 25 wt. %, OH value 40 mg KOH/g-resin, Acid value 30 mg KOH/g-resin). Thinner was used as a diluent. Acetone, ethanol (purchased from Merck), and deionized water were used to degrease and clean the metallic substrate before coating. St37 steel samples were prepared to a size of 1×25×50 and 1×100×100 mm and were used for coating and corrosion testing. The steel samples were mechanically prepared to remove the oxide layers and level the conditions of the samples and were polished with 100, 220, 400, 600, and 800 sandpaper and washed with deionized water. Before coating, the surface of the samples was degreased with acetone and ethanol and air-dried. The spray method was used to apply different coatings. In this regard, the mixture of coatings was transferred to the spray chamber. The coating was applied at a 45^{o}. After coating, the samples were dried at room temperature for 24 hours and then stored in a desiccator with a dry medium. The procedure is summarized in Figure 1.

2.2. Preparation of organic coating for electrochemical characterization

First, the resin and its hardener were mixed in a weight ratio of 10: 1.26, and this stirring was performed using mechanical stirring, and dilution at 20 % of the total weight was done using a thinner. Under these conditions, the sample was coated. The resulting coating thickness was 120 μm.

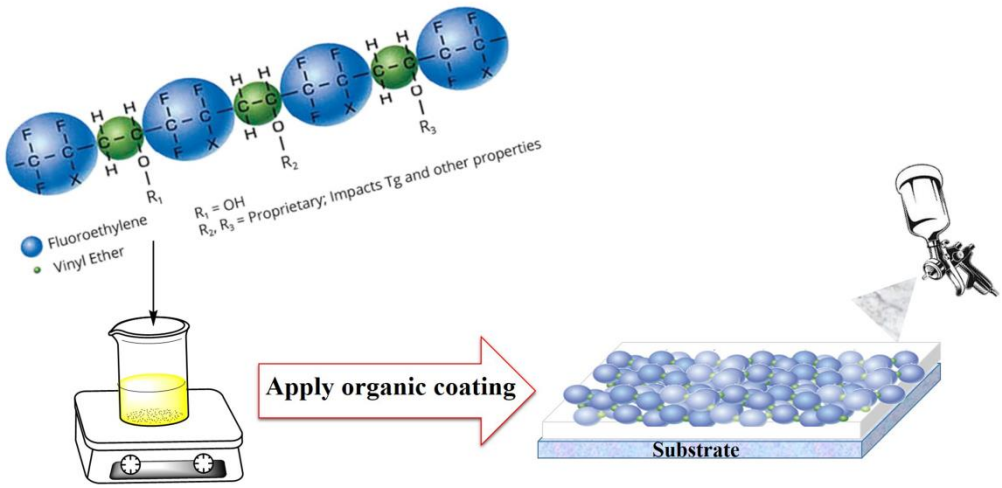

Figure 1: Schematic of FEVE coating on steel substrate.

2.3. Electrochemical and mechanical characterization

The adhesion of the coating to the substrate was tested by pull-off test according to ASTM D3359 or ASTM D 4541-02. The morphologies of the sample were also characterized using the FESEM analysis in the mode of secondary electrons (Mira3, TESCAN). The resistance determination test in the salt fog cabin was performed according to the standard method of ASTM B117 and using the salt fog cabin made by Erichsen model 606. The samples' edges and back were coated with a unique coating material and glue. Then, samples were placed inside the machine. Next, scratches of 30 mm in length and 1 mm in width are made crosswise with a sharp angle (between 30 to 45^{o}) at the bottom of coated specimens. The samples were placed at an angle of 30^{o} to the vertical line inside the salt fog cabin. Finally, the blistering effects of the coating surface were evaluated according to the ASTM D1654 standard. In addition, the corrosion effects on the substrate surface were evaluated according to ASTM D610 standard method in the scratch area and the areas away from scratches. A scratch or pencil hardness tester was used To determine the hardness and scratch-resistance of the coating applied to the steel substrate following ASTM D3363. The pencil hardness size was presented qualitatively, and a scale with a range of 6B was used as the lowest hardness, up to 9 h, which indicated the highest hardness obtained from this test. The ASTM D3363 provides manual testing without a retainer, but a pencil hardness tester made the test results reproducible. Polarization electrochemical tests measured the following tests: corrosion potential (E_{corr}), corrosion current density (i_{corr}), polarization resistance (R_p), and corrosion rate (CR) of steel substrate and coated substrate using Ivium Stat potentiostat/galvanostat apparatus. The corrosion cell in this test consisted of a 1 cm^2 platinum electrode as an auxiliary electrode, a silver/silver chloride electrode (Ag/AgCl) as a reference electrode, and a steel sample prepared (with and without the above coatings) (Dimensions 1×25×50 mm) was used as a working electrode. Only 1 cm^2 of the coating surface was exposed to the corrosive medium, and the rest of the sample areas (the areas inside the corrosive solution) were sealed with a combination of honey wax. First, the open circuit potential (OCP) in the System equilibrium was recorded as corrosion potential. Then, Tafel diagrams were scanned by potential scanning in -250 to 250 mV corrosion potential at a scan rate of 10 mV/min. After drawing the Tafel diagram, the corrosion current density was determined by extrapolation.

EIS test was used to evaluate the coating resistance and its protective properties. The corrosion cell in this test consists of the followings: a platinum electrode with an area of 2 cm^2 as an auxiliary electrode, a silver/silver chloride electrode (Ag/AgCl) as a reference electrode, a prepared steel sample (with and without the above coatings) (with dimensions of 1×25×50 mm) as a working electrode, and the used 3.5 wt. % NaCl electrolyte as a corrosive solution. Only 1 cm^2 of the coating surface was exposed to the corrosive medium, and the rest of the sample surface (areas inside the corrosive solution) was sealed with a combination of honey wax. EIS test was performed for

two, four, and eight weeks after immersion. The EIS test was performed in OCP in the frequency range of 100 kHz to 10 mHz and the sinusoidal voltage range of 10 mV. Three FEVE samples, F2, F4, and F8, which were immersed in 40 mL of salt electrolyte (3.5 wt. % NaCl solution) for 2, 4, and 8 weeks, were subjected to EIS testing. All EIS tests were performed at room temperature. EIS data were measured using Ivium software, and the data were fitted with ZSimDemo and Zview software.

The QUV tester simulated the harmful effects of long-term outdoor exposure to materials and coatings by placing test specimens in various UV, humidity, and heat conditions. Fluorescent, xenon, and carbon lamps generate a radiation spectrum within the UV wavelength range inside the chamber. UV resistance test was performed using the ASTM D5071 standard. A xenon lamp with a radiation intensity of 365 W/m^2 was used to generate UV radiation in this test. The test was performed for 120 hours, and a combination of wet and dry cycles was performed for this purpose, with a wet cycle time of 1 hour and a dry cycle of 2 hours.

3. Results and Discussion

3.1. EIS measurement

Steel samples coated with fluoroethylene vinyl ether (F) which were immersed in corrosive saline solution were subjected to EIS test after 2, 4, and 8 weeks from the time of immersion, and the results were in the form of bode diagrams and phases which were shown in Figure 2 and Table 1. To interpret the diagrams obtained from F coatings, two parameters $|Z|_{10\,mHz}$, the phase angle at the maximum frequency (100 kHz) was discussed.

As mentioned above, the value of $|Z|_{10\,mHz}$ Which is the same as the total resistance at the minimum frequency and is an excellent criterion for comparing the samples' corrosion resistance [16]. As shown in Figure 2 and Table 1, the value (log ($|Z|_{10\,mHz}$)) for F2 sample, which was related to the two-week immersion of fluoroethylene vinyl ether coating, was 7.35. The value of the log ($|Z|_{10\,mHz}$) for the F4 sample was slightly 7.27 and then, with increasing immersion time, log ($|Z|_{10\,mHz}$) for the F8 sample with a very slight increase to 7.45. The stability and no reduction in overall resistance of this coating indicated the appropriate protection function.

Examination of the results for θ_{100kHz} or the phase angle at the maximum frequency (100 kHz) of the F sample is shown in Figure 2 and Table 1. The result showed that $\theta_{100kHz,}$ at the beginning and the interval of 2 to 4 weeks of immersion in corrosive solution increased from 73.66 to 83.9. Then with increasing immersion time to 8 weeks, this amount decreased to 79.42. The absence of a significant drop in the value of θ_{100kHz} indicated the maintenance of coating adhesion during the test immersion. It was attributed to the barrier protection of the coating and the formation of protective films in the interface of metal/coating [15, 17, 18].

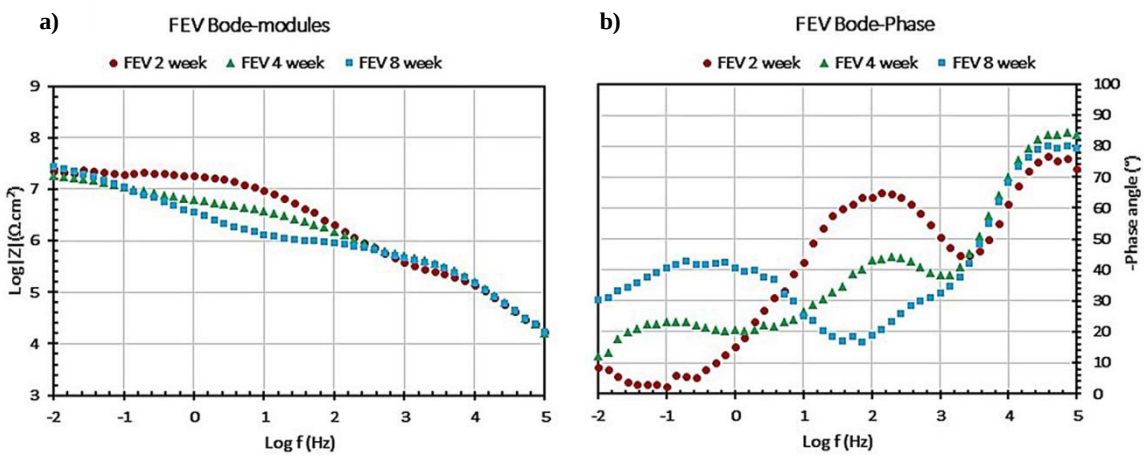

Figure 2: Bode-modulus (a), phase diagrams (b) for steel samples with fluoroethylene vinyl ether (F) coating immersed in NaCl 3.5 wt.% solution (for 2, 4, and 8 weeks).

Table 1: The values of the total impedance $|Z|_{10\ mHz}$, the phase angle at the maximum frequency ($-\Theta_{100\ kHz}$) from the EIS test related to the coating F at different immersion times (2, 4, and 8 weeks).

Sample	$-\Theta_{100kHz}$ (°)	log ($\|Z\|_{10\ mHz}$/Ω.cm^2)
F2	72.66	7.35
F4	83.9	7.27
F8	79.42	7.45

Figure 3 shows the Nyquist diagrams of the uncoated and FEVE-coated steel substrate in a 3.5 wt. % NaCl aqueous solution. In this experiment, the larger the semicircle, the higher the R_{ct} value, which means that the longer ion diffusion path from the aqueous solution to the metal substrate is longer. According to Figure 3, at 8 weeks of immersion, the charge transfer resistance was the highest, attributed to the excellent barrier effect and corrosion product, which reduced the permeability to corrosive substances. In immersion time of 4 weeks, the value of the semicircle diameter in the diagrams shows the attenuation process, which shows that the corrosion resistance of the coatings gradually decreases. When the immersion time reaches 2 and 4 weeks, a second capacitive arc appears in the Nyquist curve of the coating, meaning a two-time constant seems, indicating that the corrosion process has entered the middle stage. The corrosive medium had penetrated the layer. In Figure 3, although the two-time FEVE coating constant appeared during the fourth week of immersion, the value of the impedance modulus at the lowest frequency did not decrease significantly, indicating long-term excellent corrosion resistance. The stable main chain's high fluorine content (more than 20 %) enables the FEVE coating to maintain excellent anti-corrosion properties. The equivalent circuit in Figure 4 can be used for the initial corrosion of the FEVE coating. At this time, the hydrophobic properties of the coating surface and the internal dual crosslinking system will be useful in preventing water absorption. The corrosion medium had not penetrated the coating and had not reached the surface of the metal substrate. The equivalent circuit in Figure 4 was applicable for the medium corrosion stage after two weeks of immersion of the FEVE coating. At this time, the corrosion medium penetrates the interface between the coating and the metal substrate, and an electrochemical reaction occurs on the surface of the metal substrate, leading to corrosion. Table 2 compares the corrosion parameters of this paper and other similar work. However, most fluoropolymers have not shown outstanding corrosion resistance compared to acrylates, epoxies, and polyurethanes. Therefore, these materials are promising for multifunctional coatings and need further study to achieve high anti-corrosion performance. In particular, organic nanocomposites containing covalent coupling molecules enhance anti-corrosion performance.

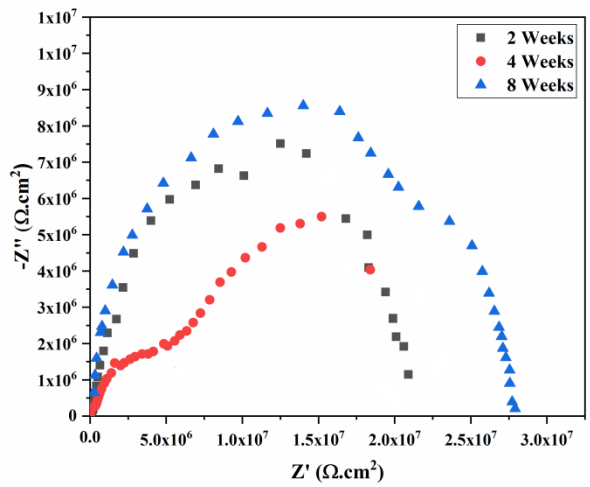

Figure 3: Nyquist plots of FEVE coating under various immersion conditions.

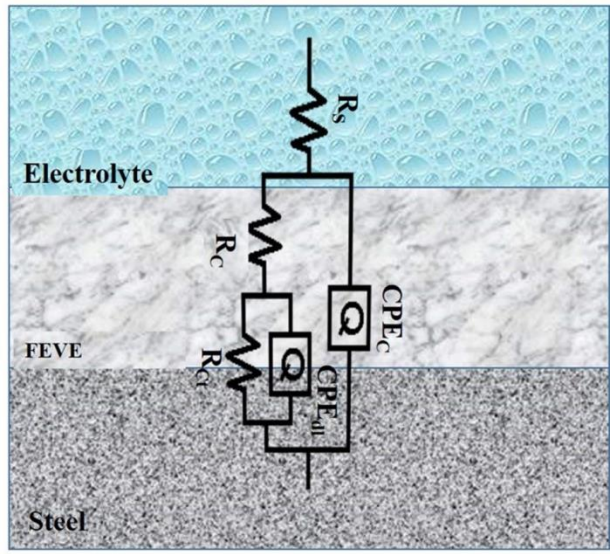

Figure 4: The equivalent circuits fit the EIS results with a two-time constant.

Table 2: Comparison of the corrosion resistance of coatings investigated in previous reports with the coating presented in this study.

Polymer matrix	Exposures	Corrosion resistance ($\Omega.cm^2$)	Reference
FEVE	1 day	2×10^5	[12]
FEVE	1 day	1.8×10^7	[19]
	2 weeks	5.0×10^6	
FEVE	2 Week	2.2×10^7	This work
	8 weeks	2.8×10^7	

Table 3: Parameters obtained from the polarization curves.

Sample	E_{corr} (V vs. Ag/AgCl)	i_{corr} (mA/cm^2)	C.R.(mm/year)
F	-0.1	6.3×10^{-7}	7.31×10^{-6}
Steel	-0.08	3.16×10^{-2}	0.366

3.2. Polarization curves

Figure 5 shows the polarization curves of bare steel, F-coated steel substrate after 8 weeks of immersion in a corrosive salt solution of 3.5 wt. % NaCl. The open-circuit potential of the system in the steady-state was considered as the corrosion potential (E_{corr}), and the corrosion current density (i_{corr}) was obtained by extrapolating the linear region of the polarization curve (Tafel zone) to the E_{corr} curve. Also, the corrosion rate (CR) in millimeters per year (mm/year) was obtained according to the following reaction (Eq. 1) [16]:

$$C.R=3.27\times\frac{i_{corr}}{\rho}\times E_w \quad (1)$$

In this regard, i_{corr}, ρ, and E_w are the density (mA/cm^2) of the current density of steel (7.87 g /cm^3) and the mass equivalent of carbon steel (27.93 g), respectively [20]. The parameters obtained from the polarization curves are presented in Table 3.

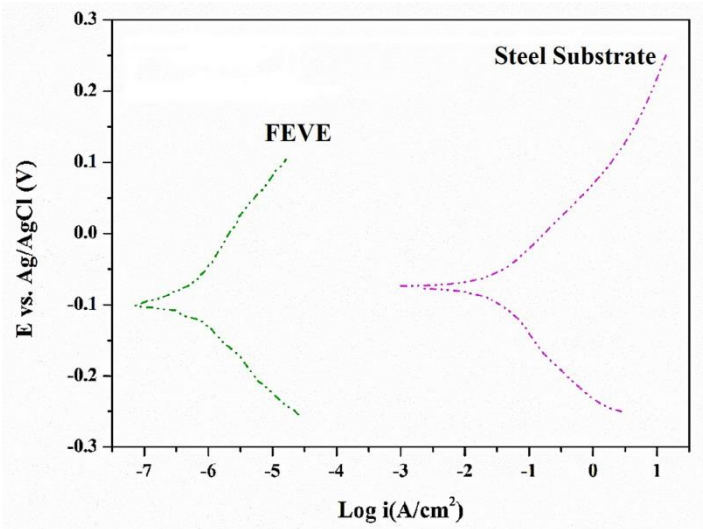

Figure 5: Polarization curve of coating F and substrate in corrosive saline solution 3.5 % by weight NaCl after 8 weeks.

As can be seen from comparing the corrosion rate of uncoated St37 steel with F-coated steel specimens, this coating significantly reduced and protected the corrosion rate of steel in a corrosive environment. Therefore, it can be concluded that if the F coating was applied, the corrosion life of the steel was significantly increased. As can be seen from Figure 5 and Table 3, although the coated sample of F was immersed in a corrosive saline solution for eight weeks, it retained its protective properties well. Therefore, the induction of barrier protection capability in the F coating used in this article ensured the long-term durability of the steel substrate against uniform corrosion in corrosive salt environments [17, 21-24]. Comparing the corrosion life of F in Table 3, this can be stated which coating had a barrier protection mechanism and showed good protective performance in the corrosive environment.

3.3. Corrosion protection mechanism

The FEVE composite had a long-term protective function based on the electrochemical studies and salt spray test results. Good corrosion protection was assigned to blocking the diffusion path of the corrosive agents into the coating. The other significant effect of the FEVE coating was twisting and increasing the diffusion path of the corrosive agents in the polymer coating and retarding the electrochemical corrosion reactions (Figure 6). Also, as shown in Figure 7, the cross-section of the coating exhibited a defect-free coating that provides barrier protection to the coating.

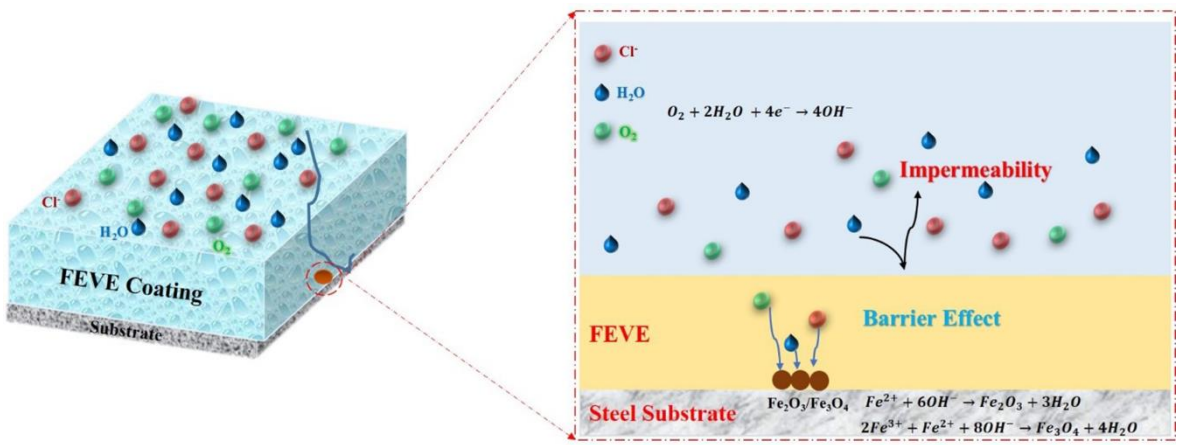

Figure 6: FEVE coating barrier protection mechanism.

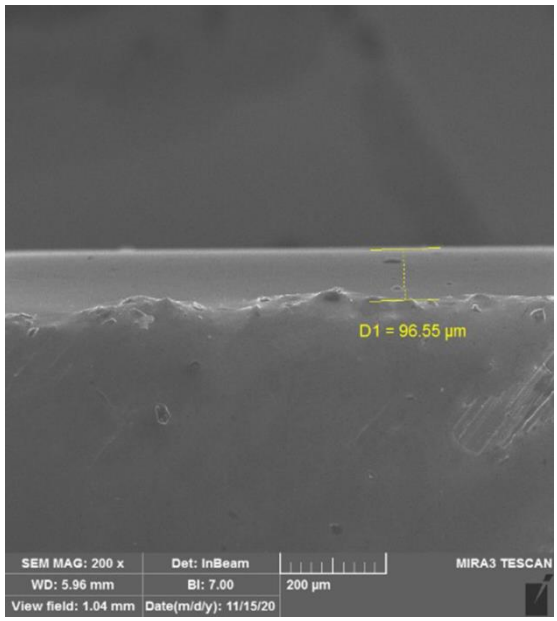

Figure 7: Cross-section of FEVE coating on steel substrate.

3.4. Adhesion test

The adhesion of F coatings to the steel substrate was evaluated by the pull-off method, and its adhesion strength was 100 psi (Figure 8). These results were completely consistent with the results of the impedance phase test. From the adhesion test results and phase curve in impedance, it can be concluded that coating F showed excellent adhesion and mechanical properties.

3.5. Salt spray test

According to ASTM B-117, the salt spray test is a way to evaluate the performance of the coating in corrosive environments. Humidity test according to ASTM D4585-07 standard; degree of scaling (ASTM D-610), degree of blistering (ASTM D-714) was performed. For this purpose, coated samples with artificial damage in the device's chamber (cabinet) were placed under a salt spray created by spraying a corrosive salt solution with high humidity. The salt spray test is a qualitatively accelerated corrosion test in which the protective performance of the coating (which contains or is free of an artificial defect) is determined by the dimensions and distribution of the degraded areas on the surface of the coated sample. The time elapsed in this test until the sample shows the first signs of discontinuity or is damaged. The delaminated from the coating was considered a measure of the protective performance of the coated sample. Delamination of the coating from the substrate was attributed to a reduced adhesion between the coating and the substrate. The reduction of adhesion during the test time was directly related to the volume of salt electrolyte containing corrosive components Steel in the interface. Corrosion products formed on the samples (created around artificial defects) and the presence of blisters created as a result of the accumulation of corrosion products under the coating and the distribution of blisters is a good criterion for comparing the protective performance of samples in this test [16].

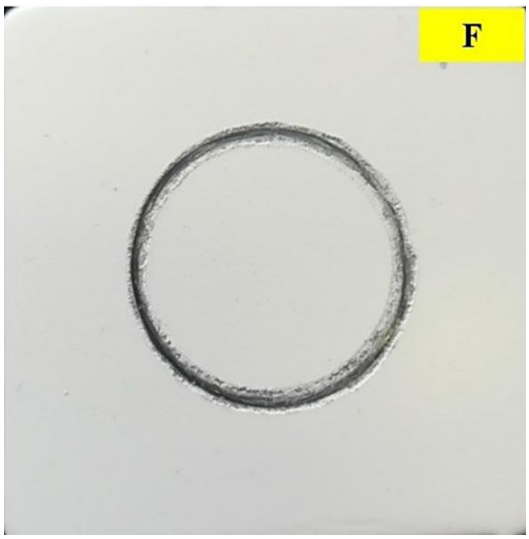

Figure 8: Pull-off adhesion test on sample F.

This study exposed a steel sample coated with fluoroethylene vinyl ether (F) to a simulated corrosive salt spray for 360 hours (Figure 9). After completing the salt spraying test, the coated steel samples were visually inspected to investigate the damaged areas. After 360, blisters were seen around the scratch area of the F coat, only very limited rust points on the surfaces, and no corrosion products were accumulated around the scratch. The results confirmed that the creation of the F coating provided excellent anti-corrosion performance for the metal substrate.

Figure 9: Salt spray test for FEVE coated steel for 360 hours.

Table 4: Coating hardness FEVE using scratch hardness method.

Sample	Degree of hardness	Hardness Range
F	H	Resiatnt

Figure 10: Hardness range of coatings in scratch or pencil hardness method.

3.6. Hardness and scratch resistance test

To determine the hardness and scratch-resistance of coating F applied on the steel substrate, the method of scratch or pencil hardness tester following ASTM D3363 standard was used. The pencil hardness test is a common method that has been used for many years in the industry to determine the coating resistance to scratches and dents [16]. The hardness magnitude in this test is qualitative, and a scale range was used from the lower stiffness of 6B up to 9H. It was indicated that the highest stiffness was obtained from this test (as shown in Figure 10). According to the test results, coating F had a good hardness and was resistant to scratches of a pencil with H hardness (Table 4).

3.7. UV weathering test

UV resistance test was performed using the ASTM D5071 standard. A xenon lamp with a radiation intensity of 365 W/m^2 was used to generate UV radiation in this test. The test was performed for 120 hours, and a combination of wet and dry cycles was performed for this purpose so that the duration of the wet cycle was equal to 1 hour, and the dry cycle was equal to 2 hours. UV resistance was evaluated by color changes, gloss stability, and thickness changes. For sample F, no change in the color and gloss of the coating was observed after 120 hours (Figure 11).

Figure 11: UV resistance test for sample F after 360 hours.

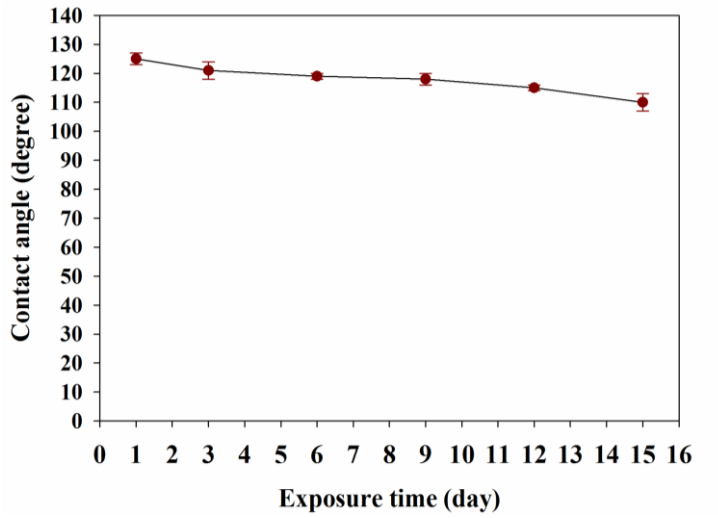

Figure 12: Variation in the contact angle on the prepared coating as a function of exposure time to UV radiation.

The excellent UV properties of the F coat were attributed to the linear chains of carbon fluoride on the surface, which provided high resistance to UV. In addition, the high electronegativity of fluorine and the polar nature of the bands make the C-F bond stronger than the C-H bond. Figure 12 showed the change in FEVE contact angle as a function of UV exposure time. After irradiation for 15 days, the wetting angle of the coating decreased from 126 to 110 °C, indicating its high UV resistance due to the presence of fluorine chains in the coating. They can effectively absorb UV radiation and reduce the degradation of surface chemical compounds.

4. Conclusion

- FEVE coating was sprayed on the surface of the St37 steel substrate.
- FEVE coatings have linear chains of carbon fluoride on the surface, which are hydrophobic, and this hydrophobicity does not decrease with increasing immersion time. Even with corrosion products present, corrosion resistance increased over time.
- FEVE samples showed excellent UV resistance. The excellent UV properties of the F model were attributed to the linear chains of carbon fluoride on the surface, which provided high resistance to UV. In addition, the high electronegativity of fluoride and the polar nature of the bands make the C-F bond more robust than the C-H bond. In addition, no corrosion products or blisters were seen on the samples for 360 hours.
- The adhesive strength of the FEVE specimen was more significant than 100 psi.
- The Scratch resistance of the sample was in the B-H range, which showed excellent scratch-resistance of the samples.

5. References

1. R. Bhaskaran, N. Palaniswamy, N. S. Rengaswamy, M. Jayachandran, A review of differing approaches used to estimate the cost of corrosion (and their relevance in the development of modern corrosion prevention and control strategies), Anti-Corros, *Methods Mater.*, 52(2005), 29-41.
2. M. Biezma, J. San Cristobal, Methodology to study cost of corrosion, *Corros. Eng. Sci. Technol.* 40(2005), 344-352.
3. J. Kruger, Cost of metallic corrosion, Uhlig's corrosion handbook, 3(2011), 15-20.
4. Y. Yang, G. Yu, J. J. Cha, H. Wu, M. Vosgueritchian, Y. Yao, Z. Bao, Y. Cui, Improving the performance of lithium–sulfur batteries by conductive polymer coating, *ACS nano*. 5(2011), 9187-9193.
5. S. M. Kang, I. You, W. K. Cho, H. K. Shon, T. G. Lee, I. S. Choi, J. M. Karp, H. Lee, One-step modification of superhydrophobic surfaces by a

mussel-inspired polymer coating, *Angew. Chem., Int. Ed. Engl.* 49(2010), 9401-9404.
6. A. Nautiyal, M. Qiao, J. E. Cook, X. Zhang, T.-S. Huang, High performance polypyrrole coating for corrosion protection and biocidal applications, *Appl. Surf. Sci.* 427(2018), 922-930.
7. W. Darden, A. C. Americas, P. Exton, P. Exton, Fluoropolymer coatings for plastics, Proceedings of the 11th Annual Coatings for Plastics Symposium, Lombard, IL, USA, (2008), 21-23.
8. A. Dreveton, Overview of the fluorochemicals industrial sectors. *Procedia Eng.* 138 (2016), 240-247.
9. H. Teng, Overview of the development of the fluoropolymer industry, *Appl. Sci.* 2(2012), 496-512.
10. R. Parker, K. Blankenship, Protective organic coatings: fluoroethylene vinyl ether resins for high-performance coatings, ASM Hand Book, AGC Chemicals Americas, 2015.
11. B. Zhong, L. Shen, X. Zhang, C. Li, N. Bao, Reduced graphene oxide/silica nanocomposite-reinforced anticorrosive fluorocarbon coating, *J. Appl. Polym. Sci.* 138(2021), 49689-49699.
12. L. Shen, H. Chen, C. Qi, Q. Fu, Z. Xiong, Y. Sun, Y. Liu, A green and facile fabrication of rGO/FEVE nanocomposite coating for anti-corrosion application, *Mater. Chem. Phys.* 263(2021), 124382-124391.
13. K. Blankenship, FEVE Powder Technology for Weather- and Corrosion-Resistant Coatings, *Focus Powder Coat.* 2020(2020), 5-11.
14. M. Joo, M. Cakmak, M. D. Soucek, Corrosion resistance of self-stratifying coatings using fluorovinyl ether/BPA epoxide, *Prog. Org. Coat.* 133(2019), 145-153.
15. M. R. Ghadimi, A. Dolati, Preparation and characterization of superhydrophobic and highly oleophobic FEVE-SiO_2 nanocomposite coatings, *Prog. Org. Coat.* 138(2020), 105388-105396.
16. M. Izadi, T. Shahrabi, B. Ramezanzadeh, Active corrosion protection performance of an epoxy coating applied on the mild steel modified with an eco-friendly sol-gel film impregnated with green corrosion inhibitor loaded nanocontainers, *Appl. Surf. Sci.* 440(2018), 491-505.
17. K. I. Aly, A. Mahdy, M. A. Hegazy, N. S. Al-Muaikel, S. W. Kuo, M. Gamal Mohamed, Corrosion resistance of mild steel coated with phthalimide-functionalized polybenzoxazines, *Coatings*. 10(2020), 1114.
18. M. Izadi, T. Shahrabi, I. Mohammadi, B. Ramezanzadeh, A. Fateh, The electrochemical behavior of nanocomposite organic coating based on clay nanotubes filled with green corrosion inhibitor through a vacuum-assisted procedure, *Compos. B. Eng.*, 171(2019), 96-110.
19. X. Wang, Y. Cui, Y. Wang, T. Ban, Y. Zhang, J. Zhang, X. Zhu, Preparation and characteristics of crosslinked fluorinated acrylate modified waterborne polyurethane for metal protection coating, *Prog. Org. Coat.* 158(2021), 106371.
20. Y. Singhbabu, B. Sivakumar, J. Singh, H. Bapari, A. Pramanick, R.K. Sahu, Efficient anti-corrosive coating of cold-rolled steel in a seawater environment using an oil-based graphene oxide ink, *Nanoscale*. 7(2015), 8035-8047.
21. K. I. Aly, M. G. Mohamed, O. Younis, M. H. Mahross, M. Abdel-Hakim, M. M. Sayed, Salicylaldehyde azine-functionalized polybenzo-xazine: Synthesis, characterization, and its nanocomposites as coatings for inhibiting the mild steel corrosion, *Prog. Org. Coat.* 138(2020), 105385.
22. K. I. Aly, O. Younis, M. H. Mahross, E. A. Orabi, M. Abdel-Hakim, O. Tsutsumi, M. G. Mohamed, M. M. Sayed, Conducting copolymers nanocomposite coatings with aggregation-controlled luminescence and efficient corrosion inhibition properties, *Prog. Org. Coat.*, 135(2019), 525-535.
23. M. G. Mohamed, A. Mahdy, R. J. Obaid, M. A. Hegazy, S. W. Kuo, K. I. Aly, Synthesis and characterization of polybenzoxazine/clay hybrid nanocomposites for UV light shielding and anti-corrosion coatings on mild steel, *J. Polym. Res.*, 28(2021), 1-15.
24. S. B. Ulaeto, R. Rajan, J. K. Pancrecious, T. Rajan, B. Pai, Developments in smart anticorrosive coatings with multifunctional characteristics, *Prog. Org. Coat.*, 111(2017), 294-314.

How to cite this article:
M. Mirzaee, M. Rezaei Abadchi, A. Mehdikhani, N. Riahi Noori, A. Zolriasatein, Corrosion and UV Resistant Coatings Using Fluoroethylene Vinyl Ether Polymer. Prog. Color Colorants Coat., 16 (2023), 47-57.